Graft Polymerization of Vinyl Acetate onto Silica

Van Nguyen, Wayne Yoshida, Yoram Cohen

Department of Chemical Engineering, University of California, Los Angeles, California 90095-1592

Received 15 January 2002; accepted 22 April 2002

ABSTRACT: The free-radical graft polymerization of vinyl acetate onto nonporous silica particles was studied experimentally. The grafting procedure consisted of surface activation with vinyltrimethoxysilane, followed by free-radical graft polymerization of vinyl acetate in ethyl acetate with 2,2′-azobis(2,4-dimethylpentanenitrile) initiator. Initial monomer concentration was varied from 10 to 40% by volume and the reaction was spanned from 50 to 70°C. The resulting grafted polymer, which was stable over a wide range of pH levels, consisted of polymer chains that are terminally and covalently bonded to the silica substrate. The experimental polymerization rate order, with respect to monomer concentration, ranged from 1.61 to 2.00, consistent with the kinetic order for the high polymerization regime. The corresponding rate order for polymer grafting varied from 1.24 to 1.43. The polymer graft yield increased with both initial monomer concentration and reaction temperature, and the polymer-grafted surface became more hydrophobic with increasing polymer graft yield. The present study suggests that a denser grafted polymer phase of shorter chains was created upon increasing temperature. On the other hand, both polymer chain length and polymer graft density increased with initial monomer concentration. Atomic force microscopy–determined topology of the polymer-grafted surface revealed a distribution of surface clusters and surface elevations consistent with the expected broad molecular-weight distribution for free-radical polymerization. © 2002 Wiley Periodicals, Inc. J Appl Polym Sci 87: 300–310, 2003

Key words: poly(vinyl acetate); silica; silylation; graft polymerization; atomic force microscopy (AFM)

INTRODUCTION

Surface modification by polymers provides a unique opportunity to engineer the interfacial properties of solid substrates while retaining their basic geometry and mechanical strength. Surface engineering can be achieved by either physically adsorbing[1–3] or chemically bonding[4–15] functional polymer chains onto a substrate. Chemical bonding of functional polymers offers a unique advantage, given that the grafted polymer layer can be completely miscible with the surrounding fluid medium yet the polymer detachment is prevented because of the covalent attachment of polymer chains to the substrate.

Among various methods for covalent bonding of polymer chains onto a substrate, free-radical surface graft polymerization has emerged as a simple method of obtaining a high surface chain coverage.[13–15] This latter method usually requires surface activation by the direct attachment of initiator molecules[4–12] or by the introduction of surface active sites[13–15] (e.g., vinyl groups in surface graft polymerization of vinyl monomers). In particular, organosilane coupling agents (i.e., chloro- and alkoxysilanes) are commonly employed to introduce active sites onto inorganic oxide surfaces. For example, the modification of amorphous silica surfaces with organosilanes has been extensively studied in both gas and liquid phases for applications such as adsorption,[16–18] adhesion,[19,20] and chromatography.[21–25] Gas-phase silylation typically results in a lower conversion and is cumbersome when a large-scale silylation is desired. Liquid-phase silylation, which is of particular interest in the present work, can be performed in water or in an anhydrous environment, and the choice of solvent greatly affects the resulting silylation coverage.[26–28] Specifically, in an aqueous environment the chloro and alkoxy groups of multifunctional organosilanes undergo bulk hydrolysis and condensation, forming polysilane networks before depositing onto the substrate.[27,28] As a result, the fraction of initial surface silanols that reacts with the functional organosilane is quite small, and the silylation process is usually nonuniform and difficult to control.[28] In contrast, in an anhydrous silylation reaction (i.e., in xylene) of a hydrated silica substrate, condensation and hydrolysis between one or more functional groups of neighboring silane molecules occur mainly on the surface, with a minimal intercondensation between silane molecules in the bulk phase.[26,28,29] As a consequence, this latter technique leads to a denser and more uniform silylation coverage. In a subsequent step, the vinylsilane-modified substrate can be free-radical graft polymerized with a desired functional monomer, producing polymer chains that are chemically bonded to the substrate along with homopolymer chains in solution. In this

Correspondence to: Y. Cohen (yoram@ucla.edu).

Journal of Applied Polymer Science, Vol. 87, 300–310 (2003)

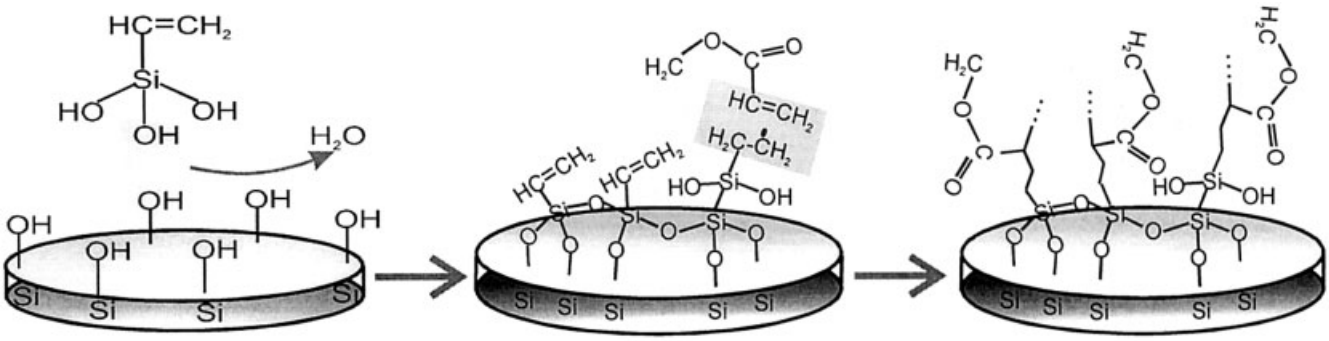

Figure 1 Surface modification of Novacite particles: (a) silylation with VTMS hydrolyzed and (b) graft polymerization with VAc.

step, the formation of grafted polymer chains is typically attributed to both propagation of growing surface chains (*surface propagation*) and coupling termination between growing homopolymer chains and growing surface chains (*polymer grafting*).[15]

Recent studies have demonstrated that silica and zirconia substrates, grafted with vinyl acetate and 1-vinyl-2-pyrrolidone, are suitable for producing low-fouling ultrafiltration membranes,[30] selective pervaporation membranes,[31] size-exclusion chromatography resins,[32] and model adsorption resins.[33] Grafting with poly(vinyl acetate) is of particular interest, in that the grafted polymer layer can render the modified substrate hydrophobic or hydrophilic [by a postgrafting hydrolysis to convert poly(vinyl acetate) into poly(vinyl alcohol) at a desired degree of hydrolysis]. In the present study, experimental results are reported for the free-radical graft polymerization of vinyl acetate (VAc) onto vinyltrimethoxysilane-modified silica particles, focusing on the effect of reaction conditions (initial monomer concentration and reaction temperature) on polymer graft yield (g grafted polymer/m^2 surface), polymer molecular weight, and grafted polymer surface density (number of grafted chains/m^2 surface).

EXPERIMENTAL

Surface graft polymerization of VAc onto nonporous silica particles was carried out through a two-step process: surface activation with vinyltrimethoxysilane (VTMS) followed by graft polymerization of VAc in ethyl acetate with 2,2′-azobis(2,4-dimethylpentanenitrile) (VAZO 52) initiator (Fig. 1).

Materials

Nonporous silica particles (Novacite L207-A), having an average diameter of 5 μm, were obtained from Malvern Minerals (Hot Springs, AK). The silica surface area, measured by Autosorb-1 BET nitrogen adsorption (Quantachrome, Syosset, NY), was approximately 2.2 m^2/g. Vinyl acetate (VAc) monomer, supplied by Polysciences (Warrington, PA), was 99% pure and used as received. Vinyltrimethoxysilane (VTMS) was obtained from Aldrich Chemical (Milwaukee, WI). Certified ACS-grade isomeric xylene, obtained from Fisher Scientific (Tustin, CA), was used as the solvent for the silylation process. 2,2′-Azobis(2,4-dimethylpentanenitrile) (VAZO 52), purchased from DuPont (Wilmington, DE), was employed as the initiator for V Ac free-radical polymerization. Ethyl acetate (99.9% pure) obtained from Fisher Scientific, was the solvent for the polymerization reaction. For size-exclusion chromatographic analyses, polystyrene/divinylbenzene packing (Tosohaas, Montgomeryville, PA) was used as the stationary phase and ACS-grade (99.5% pure) tetrahydrofuran (EM Industries, Gibbstown, NJ) was employed as the mobile phase. Polystyrene standards (Scientific Polymer Products, Ontario, NY) with polydispersity indices of 1.05–1.17 and number-average molecular weights of 8000–64,900 g/mol were used for chromatographic calibration. In addition to the modification of silica particles, identical procedures of silylation and graft polymerization were also performed with oxide (100) silicon wafers (Wafernet, San Jose, CA) for subsequent atomic force microscope (AFM) and contact angle measurements.

Silylation

Prior to silylation, the silica particles were immersed in a 1% HCl solution for 8 h at room temperature to remove contaminants, followed by washing and immersing in DI water for approximately 1 h to clean and hydrolyze the surface. The particles were then filtered and dried at 110°C in a vacuum oven overnight to remove excess surface water. Subsequently, the hydroxylated particles were silylated in an excess solution of 10% VTMS in xylene for 5 h. The silylation reaction was performed at 137°C in a slurry batch reactor equipped with reflux condenser and kept at 70°C, which is above the boiling point of the methanol condensation product yet below the boiling point of the silane solution. The silylated particles were later washed with a large volume of xylene solvent to re-

move adsorbed silane molecules, followed by drying at 150°C in a vacuum oven for 2 days to remove the remaining solvent.

Graft polymerization

Free-radical graft polymerization of VAc onto VTMS-modified silica particles, initiated by a 0.03 *M* initial concentration of VAZO 52 initiator, was carried out in a water-jacketed slurry batch reactor in which the reaction temperature was controlled to within ±0.1°C by use of a circulating water bath (Neslab Instruments, Portsmouth, NH). The reaction was conducted under a nitrogen blanket to exclude oxygen, which is known to be a strong radical scavenger. Grafting reactions were performed at initial monomer concentrations of 10, 25, and 40% by volume and reaction temperatures of 50, 60, and 70°C. It was found that an initial monomer concentration higher than 40% by volume led to a rapid conversion and a poor temperature control, making the measurements unreliable. Grafting the polymer above 70°C was not feasible because of a rapid volatilization of the ethyl acetate solvent (T_{bp} = 77°C) accompanied by a relatively high rate of conversion.

Each grafting experiment was performed by adding the VTMS-modified particles into a predetermined volume of VAc/ethyl acetate solution. The slurry mixture was then heated to a desired temperature followed by addition of the VAZO 52 initiator. To monitor conversion and polymer graft yield, 2-mL aliquots of the reaction mixture were regularly withdrawn and analyzed over the duration of the reaction. Each sample, consisting mainly of ethyl acetate, VAc, PVAc homopolymer, and PVAc-grafted silica particles, was immediately quenched with an ample amount of ethyl acetate and subsequently filtered with a 1.0-μm polyester membrane (Nuclepore Corp., Pleasanton, CA) to separate the particles from the withdrawn sample. Filtered particles were then thoroughly washed with ethyl acetate to remove physically adsorbed monomer and homopolymer and then dried in a vacuum oven at 110°C for subsequent TGA analyses.

The conversion of monomer into polymer was determined by UV spectral analysis (HP 8452A Diode Array Spectrophotometer; Hewlett–Packard, Palo Alto, CA) of the withdrawn solution. The UV absorption peak at 202 nm, which corresponds to the vinyl group, is expected to decrease as VAc is incorporated into PVAc (i.e., one vinyl group per one VAc molecule added to a PVAc chain). On the other hand, the UV absorption peak at 196 nm, which is attributed to the carbonyl group, should not decrease during the polymerization process. Therefore, taking the carbonyl group as an internal standard, the ratio of absorbance at 202 nm to that at 196 nm is related to the ratio of monomer concentration to polymer concentration in the reaction mixture. Accordingly, monomer conversion can be calculated from

$$\text{Conversion}_t = 1 - \frac{[M]_t}{[M]_0} = 1 - \left(\frac{A_{202\text{ nm}}}{A_{196\text{ nm}}}\right)_t \left(\frac{A_{196\text{ nm}}}{A_{202\text{ nm}}}\right)_0 \quad (1)$$

where t denotes the reaction time, 0 designates the initial condition, $[M]$ is the monomer concentration, and A is the absorbance. The accuracy of the above approach was verified against a gravimetric analysis of polymer conversion.

Polymer molecular weight

Molecular weight of the homopolymer was determined by size-exclusion chromatography (SEC) by use of an Isco 2350 pump (Isco Inc., Lincoln, NE) equipped with an Isco 2360 flow controller and a Valco C6W syringe loading sample injector (Valco Instrument, Houston, TX). A BioRad 1750 refractive index monitor (BioRad Digilab Division, Cambridge, MA) was used as the detector. Stainless steel chromatographic columns 30 cm length and 0.78 cm ID were obtained from Tosohaas. All chromatographic analyses were performed with polystyrene/divinylbenzene packing as the stationary phase and ACS-grade tetrahydrofuran as the mobile phase.

Surface chemical analysis

Surface-bonded VTMS and surface-grafted PVAc were detected with diffuse reflectance infrared Fourier transform (DRIFT) spectroscopy (BioRad Digilab Division). The DRIFT spectrum of silylated particles was obtained by subtracting the DRIFT spectrum of the native, unsilylated particles. Similarly, the DRIFT spectrum of PVAc-grafted particles was obtained by subtracting features attributed to the VTMS layer. Both spectra were quantified in terms of the Kubelka–Munk unit.

The amounts of grafted VTMS and PVAc were measured by thermogravimetric analyses (TGA). Specifically, each sample was first held at 110°C for 10 min to remove surface water and was then heated at a constant rate of 25°C/min to 700°C, a temperature that has been demonstrated to be sufficiently high to remove all surface-bonded organosilanes.[13] The weight-loss profiles were observed to reach a plateau quickly at the beginning of the 110°C drying period, indicating the removal of surface water before the start of the heating ramp. A second plateau in weight loss was also observed as the temperature reached 700°C, indicating the detachment of all grafted polymer chains. The amount of surface VTMS was taken as the weight difference between the VTMS-modified sample and the unmodified sample. Similarly, the amount of

grafted polymer was determined from the weight difference relative to the VTMS-modified sample.

Surface hydrophobicity

Surface hydrophobicity of PVAc-grafted wafers that had been prepared similarly to the polymer-grafted Novacite particles was studied through the use of advancing and receding contact angle measurements at a relative humidity of 65% and 22°C. Before the measurements, each wafer was cleaned according to the following sequence: three times with ethanol, two times with water, one time with ethanol, and three times with water. The wafer was subsequently oven-dried under vacuum for 30 min at 120°C and immediately placed in a sealed chamber. Measurements were conducted with DI water and diiodomethane (DIM) by use of the sessile drop method[34] with a Kruss Model G-23 contact angle instrument (Hamburg, Germany). Each reported contact angle datum is the average of four separate drops on different areas of a given surface. The size and volume of the drops were kept approximately constant (within a fraction of 1 ml) reduce variations in contact angle measurements.[35–37] The repeatability of contact angle measurements was within ±2°.

Surface topology

Surface structural features of the native oxide (100) silicon wafer and those that had been cleaned, silylated, and graft polymerized by the identical procedures employed for the Novacite particles were compared through use of a Multimode atomic force microscope (AFM) equipped with a Nanoscope IIIa SPM controller and operated in the tapping mode (Digital Instruments, Santa Barbara, CA). AFM images for native, silylated, and PVAc-grafted wafers with dimensions of 5 × 5, 1 × 1, and 0.2 × 0.2 μm were all taken under ambient air. To exclude image artifacts, trace and retrace scans were performed and compared for all samples (where trace and retrace scans are from left to right and right to left, respectively). Further, a 90° rotation of the scan direction was also performed for each sample to identify directionally dependent features or artifacts (and to optimize scan parameters as needed). In addition, images for each sample were compared after multiple scans to ascertain that there was no damage or alteration to the surface topology. The root-mean-square (R_{rms}) surface roughness was averaged from four to seven samples (all with the dimension of 5 × 5 μm) on different areas of the wafer:

$$R_{rms} = \sqrt{\frac{\sum_{i=1}^{N} (z_i - \bar{z})^2}{N - 1}} \quad (2)$$

where z_i is the height at the ith location on the scanned surface, $\bar{z}$ is the mean height of all the measured surface locations and N is the sample size.

RESULTS AND DISCUSSION

Elemental surface analysis

The presence of surface-grafted VTMS is evident from the DRIFT spectrum of the silylated particles shown in Figure 2. The spectrum reveals two peaks at 1603 and 1411 cm^{-1}, which are characteristics of the C═C bond introduced by the covalently bonded VTMS molecules.[38–40] Further, a series of small peaks near 3000 cm^{-1}, corresponding to the C—H bond stretching of the vinyl and methyl groups, are also features that are foreign to the native Novacite particles and attributed to VTMS.[38–40] AFM images confirmed that the native wafer was relatively smooth, with R_{rms} = 0.19 nm (Fig. 3). In contrast, the silylated wafer is rougher (R_{rms} = 2.17 nm) and contained noticeable clusters 10 to 20 nm in height and 22 nm in diameter and separated on the average by about 50 nm (Fig. 3). Fractal dimension analyses of the silylated wafers suggest that these clusters are distributed randomly with a continuous size distribution. In addition, they appear to have smooth edges and do not result from aggregation of smaller clusters. These clusters are believed to be local polysilane networks grown on the surface, resulting from the intermolecular condensation of neighboring VTMS molecules. TGA measurements indicate an average VTMS surface density of 13 vinyl groups/nm^2 (~ 22.4 μmol/m^2), which is nearly three times higher than the maximum silanol density of 4.6 groups/nm^2 on a fully hydroxylated silica surface,[41–44] also indicating the formation of polysilane structures.

The DRIFT spectrum of the PVAc-grafted particles also displays a series of small peaks around 3000 cm^{-1} corresponding to the C—H bond stretching of the hydrocarbon backbone of the grafted polymer chains (Fig. 2). In addition, the ester group introduced by the VAc monomer is clearly noticeable as indicated by the C═O bond stretching at 1744 cm^{-1}, and a group of partially overlapped peaks at 1213–1088 cm^{-1}, attributed to the C—O bond stretching.

The stability of the silylated and PVAc-grafted surfaces were also tested over a wide range of pH conditions. Stability experiments were conducted by immersing the modified particles into well-stirred solutions of different pH levels for 336 h. As an example, the remaining mass of each of the silylated samples (with an average silylation yield of 22.4 μmol VTMS/m^2) differed by at most 5% relative to the reference sample, whereas the mass variations for the PVAc-grafted particles ([M_0] = 10% and T = 60°C) were all within 8% (Fig. 4). Clearly, all the observed variations are within experimental uncertainty, confirming the

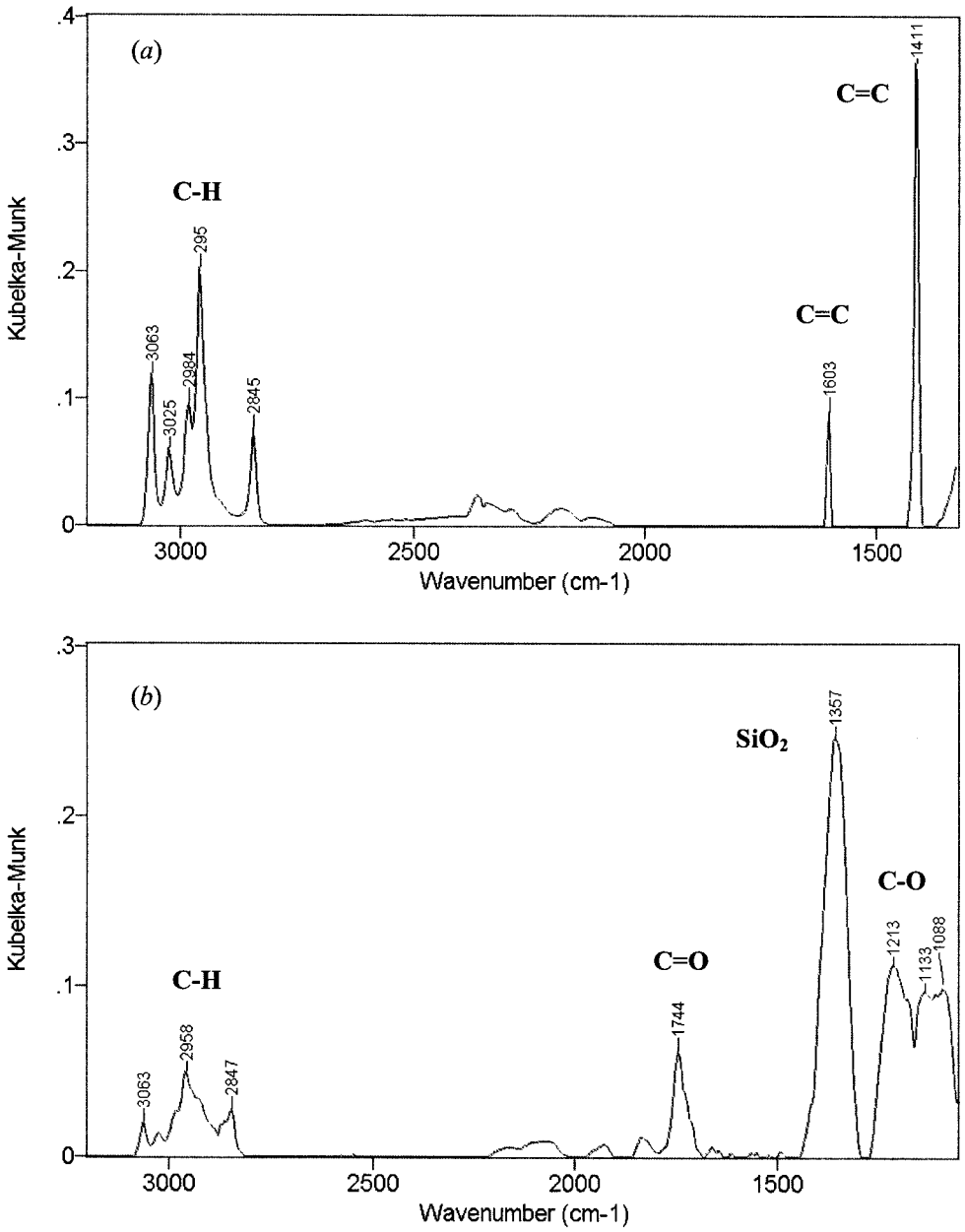

Figure 2 DRIFT spectra of (a) silylated silica particles (silylation yield = 22.4 μmol/m^2) and (b) PVAc-grafted particles ([M_0] = 10%, T = 60°C).

stability of both the silylated and grafted PVAc layers under various pH conditions.

Monomer conversion and polymer graft yield

Monomer conversion increased with temperature, consistent with the expected increase in reactivity of various species in the reaction mixture (Fig. 5). In addition, conversion also increases with initial monomer concentration, as expected for free-radical polymerization. Given that the conversion reported in Figure 5 includes monomer consumed in both homopolymerization and graft polymerization reactions, the total rate of polymerization (R_p, mol L^{-1} min^{-1}) can be written as[15]

$$R_p \equiv -\frac{d[M]}{dt} = k_p([M_n\cdot] + [S_n\cdot])[M] \qquad (3)$$

where k_p (L mol^{-1} min^{-1}) denotes the rate coefficient for polymer chain propagation, [M] is the monomer concentration (mol/L), and [$M_n\cdot$] and [$S_n\cdot$] designate the concentrations (mol/L) of growing homopolymer chains and growing grafted polymer chains, respectively. In writing eq. (3), the standard long-chain ap-

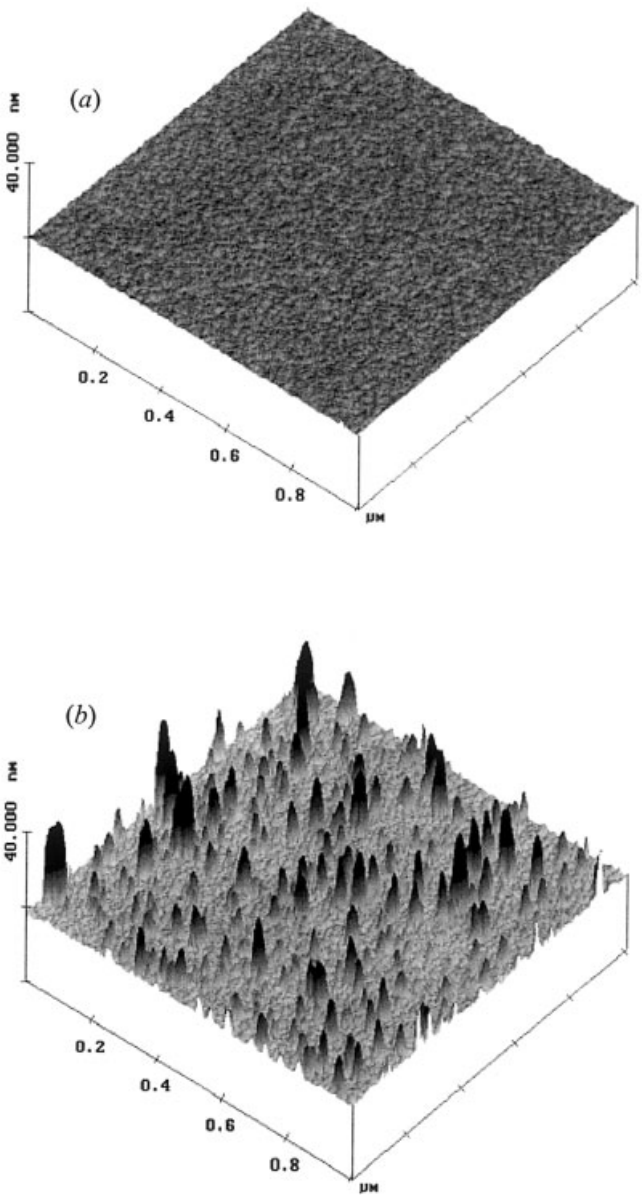

Figure 3 Tapping mode AFM images of (a) native silicon wafer and (b) silylated silicon wafer (silylation yield = 22.4 μmol/m^2).

proximation was invoked for both the free and grafted polymer.[15] For the present system, as in most typical graft polymerization processes, the initial monomer concentration is significantly higher than the initial surface VTMS concentration (on a volume basis). Therefore, it is expected that $[M_n \cdot] \gg [S_n \cdot]$ throughout the grafting process, and the overall rate of polymerization can be approximated by the rate of homopolymerization (R_h):[15]

$$R_p \approx R_h = k_p[M_n \cdot][M] \tag{4}$$

In general, the rate of homopolymerization can be written as[45]

$$R_h = k_m[I]^\alpha[M]^\beta \tag{5}$$

in which k_m denotes the overall rate coefficient for homopolymerization and $[I]$ is the initiator concentration. In classical free-radical homopolymerization, when the initiator concentration is sufficiently low, the rate of initiator–polymer termination is negligible compared to the rate of polymer–polymer termination, $\alpha = \frac{1}{2}$ and $\beta = 1$.[46] However, when the initiator concentration is sufficiently high termination of polymer radicals occurs predominantly with initiator radicals, and thus $\alpha = 0$ and $\beta = 2$.[47] When the rates of initiator–polymer termination and polymer–polymer termination are comparable, α ranges from 0.5 to 0.0 as β varies from 1 to 2.[45]

In the present study, the initial initiator concentration was the same for runs. Moreover, given the approximation of a reasonably constant intiator concentration over the course of the experiment, for the present level of intiator loading, the rate of polymerization was thus fitted to the kinetic monomer conversion data by the following expression:

$$R_p = k'_m[M]^\beta \tag{6}$$

where k'_m and β are the apparent (overall) rate coefficient and rate order (with respect to monomer concentration) for homopolymerization. It is noted that, whereas the rate coefficient k'_m is expected to depend only on temperature, the apparent rate order β can change with both temperature and initial monomer concentration. Therefore, the reported values of β are the averages over the monomer concentration range employed in this study. The values of k'_m and β resulting from the fits of eq. (6) to the experimental conversion data are given in Table I. The average kinetic rate

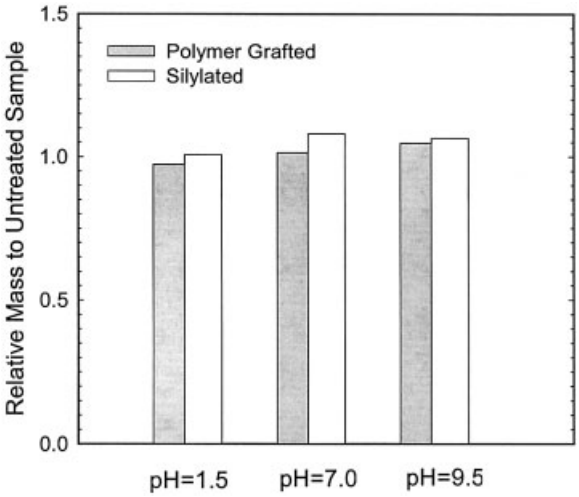

Figure 4 Remaining mass relative to untreated reference samples of silylated and PVAc-grafted Novacite particles at different pH levels ($[M_0]$ = 10%, T = 60°C).

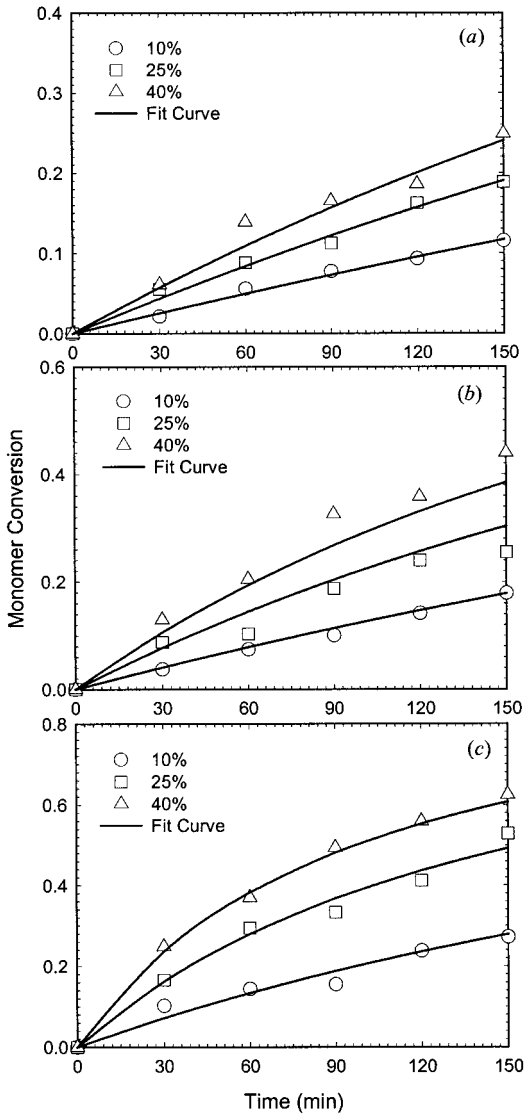

Figure 5 Experimental monomer conversion data for VAc-graft polymerization. The three curves correspond to initial monomer concentrations of 10, 25, and 40% by volume. Top (a), middle (b), and bottom (c) pictures correspond to temperatures of 50, 60, and 70°C, respectively.

order increases from 1.61 (at 50°C) to 2.00 (at 70°C), suggesting the importance of termination between the initiator and polymer radicals. This observation is consistent with the study of Ito[47] on the free-radical homopolymerization of VAc in dimethylformamide (DMF) with 2,2′-azobisisobutyronitrile (AIBN) initiator at initial monomer and initiator concentrations comparable with those in the present work.

The increase in polymer graft yield (mg grafted polymer/m^2 surface) with reaction temperature and initial monomer concentration (Fig. 6) is consistent with the increase in the rate of monomer addition to the homopolymer over the same range of conditions polymer (Fig. 5). Given that surface chain growth occurs predominantly through surface chain propagation, the overall rate of polymer grafting (g m^{-2} min^{-1}) can be approximated by[15]

TABLE I
Lumped Kinetic Parameters β, k'_m, γ, and k_{gy} for VAc Graft Polymerization

Temperature (°C)	Homo-polymerization		Graft polymerization	
	β	k'_m ($\times 10^3$)	γ	k_{gy} ($\times 10^6$)
50	1.61	0.82	1.43	2.17
60	1.73	1.33	1.38	4.00
70	2.00	2.41	1.24	8.10

$$R_{gy} \equiv \frac{d}{dt}\langle GY\rangle = \frac{k_p[S_n\cdot][M]MW_0}{(SA)(m_0)} = k_p(S_n\cdot)[M]MW_0 \quad (7)$$

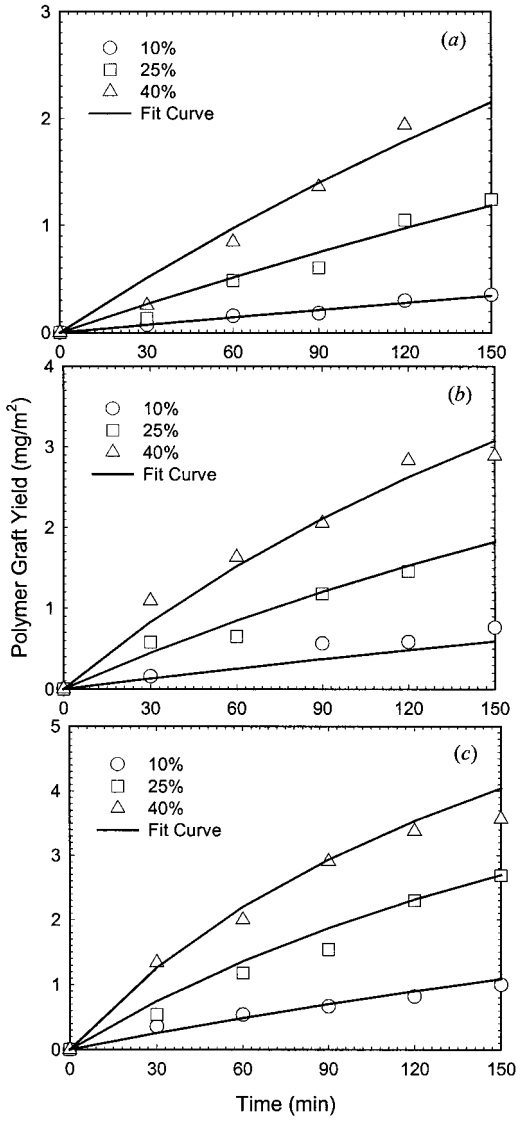

Figure 6 Experimental polymer graft yield data for VAc-graft polymerization. Data are at the same conditions shown in Figure 5.

TABLE II
Experimental Polymer Graft Yield (mg grafted polymer/m² surface), Experimental Homopolymer Number-Average Molecular Weight (g/mol), Calculated Polymer Graft Density (μmol grafted chains/m² surface), and Calculated Surface Chain Spacing for VAc Graft Polymerization onto Silica ($[I_0] = 0.03M$, $(S_n \cdot) = 22.4$ μmol/m²)

Reaction condition					
$[M_0]$ (v/v)	T (°C)	$\langle GY \rangle$ (mg/m²)	$\langle \overline{MW}_h \rangle$ ($\times 10^{-4}$) (g/mol)[a]	$\langle GD \rangle$ ($\times 10^2$) (μmol/m²)	Chain spacing D (nm)[b]
10	60	0.76	1.26 (146)	6.06	5.23
25	60	1.63	2.05 (238)	7.18	4.81
	50	2.13	4.46 (519)	4.77	5.90
40	60	2.89	2.94 (342)	9.83	4.11
	65	2.96[c]	2.61 (303)	11.33	3.83

[a] The number-average degrees of polymerization are given inside the parentheses.
[b] Calculated based on the expression $D = (\langle GD \rangle N_A)^{-1/2}$.
[c] Interpolated from the experimental polymer graft yield data at 50, 60, and 70°C.

where MW_0 designates the monomer molecular weight, SA (m²/g) is the specific area of the Novacite substrate (m²/g), m_0 (g silica/L solution) is the initial substrate loading, and $(S_n \cdot)$ is the surface density of grafted polymer chains (mol grafted chains/m² surface). A recent study on the kinetics of free-radical graft polymerization of 1-vinyl-2-pyrrolidone onto silica suggested that both the initiator radicals and the polymer radicals initiate new surface chains.[15] If the initiator radicals are the primary means of surface initiation, $(S_n \cdot)$ will increase with $[I]$ and decrease with $[M]$.[15] However, if new surface chains are initiated predominantly by the polymer radicals, $(S_n \cdot)$ will increase with $[M]$ yet it will be relatively insensitive to $[I]$. Therefore, for fixed initiator and surface VTMS concentrations, eq. (7) can be rewritten empirically as

$$R_{gy} = k_{gy}[M]^{\gamma} \tag{8}$$

where k_{gy} and γ designate the apparent rate coefficient and the apparent rate order (with respect to the monomer concentration) for polymer graft yield, respectively. Similar to the overall rate of polymerization, only the average value of γ (over the monomer concentration range studied) is considered in this work. The values of k_{gy} and γ resulting from the fits of eq. (8) to the experimental graft yield data are given in Table I. Over the present temperature range, γ, decreased by about 13% over the temperature range from 50 to 70°C, suggesting an increasing contribution of surface initiation by initiator radicals with increasing temperature.

Molecular weight, polymer graft density, and surface topology

The experimental number-average molecular weights ranged from 12,600 to 44,600 g/mol (Table II). The homopolymer molecular weight decreased with rising temperature, whereas the polymer graft yield increased over the same temperature range. As monomer concentration increases, longer polymer chains are produced as a result of a net enhancement of the rate of polymer chain propagation (i.e., data at 60°C). This latter observation is consistent with previous studies on VAc homopolymerization in methanol,[48] toluene,[49] and ethyl acetate.[49]

Experimental molecular weight data were not obtained for the grafted polymer due to the difficulty of degrafting the PVAc chains for SEC analyses. Notwithstanding, one can estimate the molecular weight of the grafted polymer, given that the size of these chains, for free-radical graft polymerization, is expected to be similar to that of the homopolymer. This assertion is supported by studies of polymer grafting onto silica,[15] glass,[50] silicon,[51] and rubber.[52–54] Accordingly, the polymer graft density ($\langle GD \rangle$) can be estimated by

$$\langle GD \rangle = \frac{\langle GY \rangle}{\langle \overline{MW}_h \rangle} \tag{9}$$

where $\langle GY \rangle$ is the polymer graft yield (g grafted polymer/m² surface) and $\langle \overline{MW}_h \rangle$ is the number-average molecular weight. As shown in Table II, the estimated polymer chain density increases significantly with temperature and, to a lesser extent, with initial monomer concentration. Apparently, for the current system a higher reaction temperature favors the formation of a denser grafted layer of shorter chains. A higher initial monomer concentration, however, enhances both the grafted chain length and the polymer graft density. The effects of temperature and initial monomer concentration on the grafted polymer layer are further evident from AFM images of the PVAc-grafted silicon wafers (Fig. 7). As the reaction temperature increased from 50 to 60°C, the grafted surface became more densely populated with smaller polymer clusters of lower molecular weights, and the root-mean-square roughness increased from 2.84 nm (at 50°C) to

3.26 nm (at 60°C). However, both the number density and the polymer cluster size increased as the initial monomer concentration increased from 25 to 40%. Nevertheless, for all grafting conditions the surface topology reveals a broad distribution of cluster sizes, which is consistent with the heterogeneity of the underlying silylated layer and the broad molecular-weight distribution expected for free-radical polymerization.

Surface hydrophobicity

The hydrophobicity of the polymer-grafted surface was assessed by contact angle measurements with water and diiodomethane (DIM) as references for the relative interactions of the modified substrate with polar and apolar solvents. With water, the advancing contact angle (θ_a) increased by 13% as the polymer graft yield increased from 0.76 to 2.89 mg/m^2 (Table III). This result suggests that at a sufficiently high polymer graft yield, the PVAc-grafted surface becomes densely populated with surface chains at sufficient density to isolate the native surface from the contacting fluid. On the other hand, the advancing contact angle (θ_a) with DIM decreased by 50% over the same range of polymer graft yield (Table III). The grafted PVAc layer has a more favorable interaction with DIM (than with water). Clearly, these results for the advancing contact angle, which is often regarded as the angle closest to the equilibrium value,[55,56] indicate a hydrophobic polymer-grafted surface.

For a real surface, several equilibrium contact angles can exist, resulting in a contact-angle hysteresis. The contact-angle hysteresis ($H \equiv \theta_a - \theta_r$), defined as the difference between the advancing angle (θ_a) and the receding angle (θ_r), can be an indication of surface roughness, surface chemical heterogeneity, penetration of liquid into the solid surface, and reorientation of surface functional groups.[57–62] The present results show that with increasing polymer graft yield the contact-angle hysteresis with water, a poor solvent for PVAc, increases, whereas it decreases with DIM, a better solvent for PVAc (Table III). It is possible that the receding contact angle (θ_r) with water is affected by the reorientation of the electron-rich ester groups of the VAc monomer units, improving the attraction between the receding water molecules and the grafted polymer chains. With DIM, the change in θ_r could be influenced by both the reorientation of the hydrophobic hydrocarbon backbones of the grafted polymer chains and some solvent penetration into the grafted polymer layer. The above characterization suggests that the molecular structure of the grafted polymer phase may play an important role in controlling surface wettability. Therefore, further research is warranted to systematically quantify the effects of surface topology on solvent wettability.

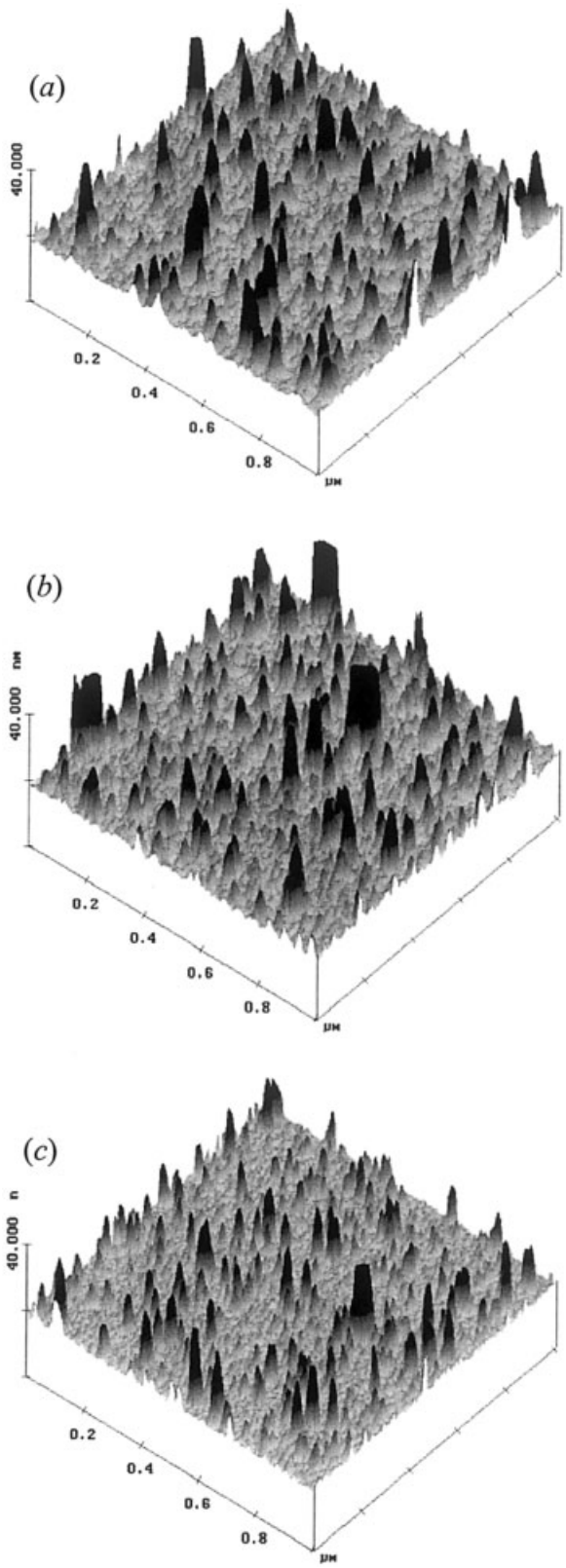

Figure 7 Tapping mode AFM images (1 × 1 micrometers) of PVAc-grafted wafers: (a) [M_0] = 40%, T = 50°C; (b) [M_0] = 40%, T = 60°C; and (c) [M_0] = 25%, T = 60°C. (Vertical scale is in nanometers).

TABLE III
Advancing Contact Angle (θ_a), Receding Contact Angle (θ_r), and Contact Angle Hysteresis ($H \equiv \theta_a - \theta_r$) for PVAc-Grafted Wafers

Polymer graft yield $\langle GY \rangle$ (mg/m^2)	Water			Diiodomethane		
	θ_a (°)	θ_r (°)	H (°)	θ_a (°)	θ_r (°)	H (°)
0.76	64	34	30	55	32	23
2.13	69	28	41	43	27	16
2.89	73	24	49	33	19	14

CONCLUSIONS

An experimental study was conducted on the free-radical graft polymerization of VAc onto nonporous silica, focusing on the effects of initial monomer concentration and temperature on structural properties of the grafted polymer phase. The apparent rate orders of homopolymerization and polymer grafting ranged from 1.61 to 2.00 and from 1.24 to 1.43, respectively. Increasing temperature enhanced the polymer graft density while reducing the polymer molecular weight. Increasing the initial monomer concentration, however, enhanced both the polymer chain length and the number of grafted chains on the surface. Surface topology was found to have a broad distribution of grafted cluster sizes, consistent with the expected broad molecular-weight distribution for free-radical polymerization. Finally, the polymer graft yield increased with both reaction temperature and initial monomer concentration, yielding a more hydrophobic PVAc-grafted surface.

The authors acknowledge the contact angle measurements by Dr. Ron S. Faibish and partial support of this work by the National Science Foundation and the U.S. Department of Energy.

References

1. Bendahl, L.; Hansen, S. H.; Gammelgaard, B. Electrophoresis 2001, 22, 2565.
2. Kanekiyo, Y.; Inoue, K.; Ono, Y.; Sano, M.; Shinkai, S.; Reinhoudt, D. N. J Chem Soc Perkin Trans 1999, 12, 2719.
3. Chen, T.-Y.; Somasundaran, P. J Am Ceram Soc 1998, 81, 140.
4. Tsubokawa, N.; Ishida, H. J Polym Sci Part A: Polym Chem 1992, 30, 2241.
5. Shelden, R. A.; Meier, L. P.; Caseri, W. R.; Suter, U. W.; Hermann, R.; Muller, M. Acta Polym 1993, 44, 206.
6. Luzinov, I.; Voronov, A.; Minko, S.; Kraus, R.; Wilke, W.; Zhuk, A. J Appl Polym Sci 1996, 61, 1101.
7. Hayashi, S.; Takamitsu, I.; Tsubokawa, N. J Macromol Sci Pure Appl Chem 1997, A34, 1381.
8. Tsubokawa, N.; Satoh, M. J Appl Polym Sci 1997, 65, 2165.
9. Prucker, O.; Ruhe, J. Macromolecules 1998, 31, 602.
10. Ejaz, M.; Yamamoto, S.; Ohno, K.; Tsujii, Y.; Fukuda, T. Macromolecules 1998, 31, 5934.
11. Velten, U.; Samuele, T.; Shelden, R. A.; Caseri, W. R.; Suter, U. W. Langmuir 1999, 15, 6940.
12. Husseman, M.; Malmstrom, E. E.; McNamara, M.; Mate, M.; Mecerreyes, D.; Benoit, D. G.; Hedrick, J. L.; Mansky, P.; Huang, E.; Russell, T. P.; Hawker, C. J. Macromolecules 1999, 32, 1424.
13. Chaimberg, M.; Parnas, R.; Cohen, Y. J Appl Polym Sci 1989, 37, 2921.
14. Browne, T.; Chaimberg, M.; Cohen, Y. J Appl Polym Sci 1992, 44, 671.
15. Nguyen, V.; Yoshida, W.; Jou, J. D.; Cohen, Y. J Polym Sci Part A: Polym Chem 2002, 40, 26.
16. Barthel, H. Chemically Modified Surfaces, 4th Proc Symp 1992, 243.
17. Fireman-Shoresh, S.; Huesing, N.; Avnir, D. Langmuir 2001, 17, 5958.
18. Fonseca, M. G.; Oliveira, A. S.; Airoldi, C. J Colloid Interface Sci 2001, 240, 533.
19. Plueddemann, E. P. Silane Coupling Agents, 2nd ed.; Plenum Press: New York, 1990.
20. Walker, P. In Silanes and Other Coupling Agents; K. L. Mittal, Ed.; VSP: The Netherlands, 1992.
21. Olieman, C.; Sedlick, E.; Voskamp, D. J Chromatogr 1981, 207, 421.
22. Grossmann, F.; Ehwald, V.; du Fresne von Hohenesche, C.; Unger, K. K. J Chromatogr A 2001, 910, 223.
23. Nakashima, K.; Fuchigami, Y.; Kuroda, N.; Kinoshita, T.; Akiyama, S. J Liq Chromatogr Relat Technol 2000, 23, 2533.
24. Sudo, Y. Bunseki Kagaku 2000, 49, 275.
25. Suzuki, S.; Kuwahara, Y.; Makiura, K.; Honda, S. J Chromatogr A 2000, 873, 247.
26. Blitz, J. P.; Murthy, R. S. S.; Leyden, D. E. J Am Chem Soc 1987, 109, 7141.
27. Van Der Voort, P.; Vansant, E. F. J Liq Chromatogr Relat Technol 1996, 19, 2723.
28. Yoshida, W.; Castro, R. P.; Jou, J. D.; Cohen, Y. Langmuir 2001, 17, 5882.
29. Hunsche, A.; Goerl, U.; Mueller, U.; Knaack, M.; Goebel, T. Kautsch Gummi Kunstst 1997, 50, 881.
30. Faibish, R. S.; Cohen, Y. Colloids Surf A 2001, 191, 27.
31. Jou, J. D.; Yoshida, W.; Cohen, Y. J Membrane Sci 1999, 162, 269.
32. Cohen, Y.; Faibish, R. S.; Rovira-Brau, M. In Interfacial Phenomena in Chromatography; Pefferkorn, E., Ed.; Marcel Dekker: New York, 1999.
33. Rovira-Brau, M.; Giralt, F.; Cohen, Y. J Colloid Interface Sci 2001, 235, 70.
34. Good, R. J. In Contact Angle, Wettability and Adhesion; K. L. Mittal, Ed.; VSP: The Netherlands, 1993.
35. Drelich, J.; Miller, J. D.; Good, R. J. J Colloid Interface Sci 1996, 179, 37.
36. Marmur, A. Adv Colloid Interface Sci 1994, 50, 121.
37. Marmur, A. Colloids Surf A: Physicochem Eng Aspects 1998, 136, 209.
38. Siberzan, P.; Leger, L.; Ausserre, D.; Benatta, J. J. Langmuir 1991, 7, 1647.
39. Tripp, C. P.; Hair, M. L. Langmuir 1992, 8, 1120.
40. Blitz, J. P.; Murthy, R. S. S.; Leyden, D. E. J Colloid Interface Sci 1988, 121, 63.
41. Iler, R. K. The Chemistry of Silica; John Wiley & Sons: New York, 1979.
42. Dong, Y.; Pappu, S. V.; Xu, Z. Anal Chem 1998, 70, 4730.
43. Chuang, I.-S.; Maciel, G. E. J PHys Chem B 1997, 101, 3052.

44. Zhuralev, L. T. Colloids Surf 2000, 173, 1.
45. Bamford, C. H.; Jenkins, A. D.; Johnston, R. Trans Faraday Soc 1959, 55, 1451.
46. Odian, G. Principles of Polymerization, 3rd ed., Wiley–Interscience: New York, 1991.
47. Ito, K. J Polym Sci Polym Chem Ed 1977, 15, 2037.
48. Kominami, T. Kogyo Kagaku Zasshi 1959, 62, 151.
49. McKenna, T. F.; Villanueva, A. J Polym Sci Part A: Polym Chem 1999, 37, 589.
50. Ejaz, M.; Tsujii, Y.; Fukuda, T. Polymer 2001, 42, 6811.
51. Yamamoto, S.; Ejaz, M.; Ohno, K.; Tsujii, Y.; Matsumoto, M.; Fukuda, T. Polym Prepr (Am Chem Soc Div Polym Chem) 1999, 40, 401.
52. Banderet, A.; Kobryner, W. C R Acad Sci III 1957, 244, 604.
53. Kobryner, W.; Banderet, A. J Polym Sci 1959, 34, 381, 394.
54. Cooper, W.; Vaughan, G.; Madden, R. W. J Appl Polym Sci 1959, 1, 329.
55. Kwok, D. Y.; Leung, A.; Lam, C. N. C.; Li, A.; Wu, R.; Neumann, A. W. J Colloid Interface Sci 1998, 206, 44.
56. Good, R. J. Surf Colloid Sci 1979, 11, 1.
57. Johnson, R. E., Jr.; Dettre, R. H. In Surface and Colloid Science, Vol. 2; E. Matijevic, Ed.; Wiley–Interscience: New York, 1969.
58. Marmur, A. Adv Colloid Interface Sci 1994, 50, 121.
59. Cassie, A. B. D. Discuss Faraday Soc 1948, 3, 11.
60. Yasuda, T.; Okuno, T. Langmuir 1994, 10, 2435.
61. Huh, C.; Mason, S. G. J Colloid Interface Sci 1977, 60, 11.
62. Hazlett, R. D. In Contact Angle, Wettability and Adhesion; K. L. Mittal, Ed.; VSP: The Netherlands, 1993.